VIP Sodium Mercury Amalgams

DOI: 10.1002/anie.201108064

$Na_{11}Hg_{52}$: Complexity in a Polar Metal**

Constantin Hoch and Arndt Simon*

Amalgams of the alkaline and alkaline-earth metals are excellent model systems for studies on polar metals. Polar metals are substances in which the transition from classical metallic bonding towards ionic bonding can be found, similar to the transition from covalent to ionic bonding in a polar atom bond. The interplay of ionic and metallic bonding leads to structures of high complexity. The most mercury-rich sodium amalgam represents an outstanding example of chemistry between salts and metals and is closely related to a very prominent process of chemical industry: the chlor-alkali process, an electrolysis on which about 50% of the total turnover of the chemical industry is based as a result of the importance of the base chemicals produced: caustic soda (soda lye; NaOH) and chlorine.[1,2] We have synthesized $Na_{11}Hg_{52}$ single crystals by combining electrolytic and thermochemical preparation methods. Its crystal structure shows motifs from closest sphere packing, cluster formation with metal–metal bonding, and Coulomb interactions between Na cations and a negatively polarized Hg sublattice. This structure, in combination with different hierarchies of over-structures and pseudo-symmetry, results in the typical physical properties of a "bad" metal.

The mercury in the amalgam plants of Western Europe (Castner Kellner cells)[3,4] constantly contain around 300–850 tons of dissolved $Na_{11}Hg_{52}$ as the most mercury-rich amalgam.[5–10] Despite its enormous impact, a detailed characterization of this amalgam was not available. In textbooks it is normally referred to as "$NaHg_x$" or "Na·Hg". The description of its synthesis by Berzelius[11] inspired Davy to prepare the first samples of elemental sodium from it by distilling off the mercury in 1807.[12] However, the solid phase which is in equilibrium with liquid mercury was first studied systematically in the early 1950s.[13,14] Thermoanalytical investigations[15] gave only very preliminary information about the mercury-richest sodium amalgam, and its composition was approximated as "$NaHg_4$". We have now determined it to be much closer to $NaHg_5$ by analysis of the single-crystal structure of $Na_{11}Hg_{52}$.

The crystal structure of $Na_{11}Hg_{52}$[16] is formed from 102 crystallographically independent Hg and 30 Na sites. All interatomic distances are in very good agreement with those found for other Na amalgams.[17] The Na atoms are coordinated by polyhedra of 14 to 16 atoms with Na–Hg distances ranging from 314(4) pm (Na11–Hg63) to 376(4) pm (Na2–Hg81). The polyhedra can be classified into four groups: four-capped pentagonal prisms, five-capped pentagonal prisms, three-capped hexagonal prisms, and double polyhedra from two interpenetrating Frank–Kasper polyhedra of 16 vertices containing two Na atoms with a shortest separation of 378(9) pm (Figure 1a).

In the cases of the capped prisms, the Na atoms are coordinated only by Hg atoms. The Frank–Kasper double polyhedra form rods parallel to the *c* axis by sharing common triangular faces. They are arranged in a slightly distorted

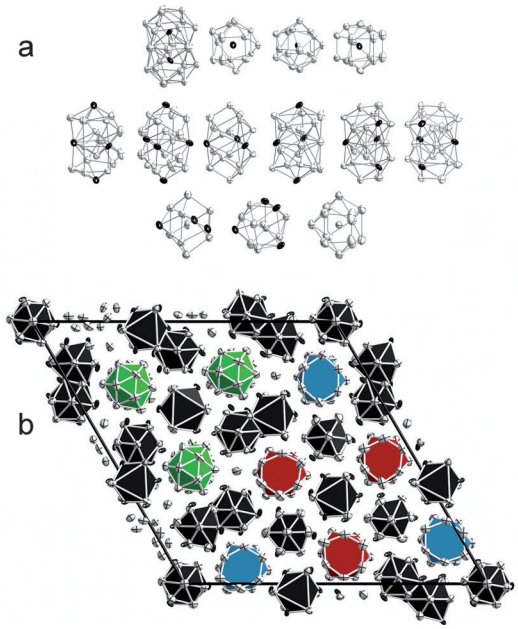

Figure 1. a) Selected coordination polyhedra around Na (upper row, from left to right: double polyhedron formed by two interpenetrating Frank–Kasper polyhedra with 16 vertices (centered by Na1), tri-capped pentagonal prism (Na7), four-capped pentagonal prism (Na4), tri-capped hexagonal prism (Na14)), and Hg (middle row, from left to right: double polyhedron from face-sharing centaur polyhedra (Hg5), interpenetrating (Hg4) and face-sharing Edshammar polyhedra (Hg25), interpenetrating icosahedra (Hg23), interpenetrating polyhedra with 13 (Hg45) and 14 vertices (Hg10); bottom row, from left to right: isolated Edshammar polyhedron (Hg67), icosahedron (Hg6), and mono-capped Edshammar polyhedron (Hg89)). b) Projection of the unit cell parallel to the *c* axis emphasizing the distorted hexagonal close packing of rods of the polyhedra around Na1 (red), Na2 (blue), and Na3 (green) and their respective surrounding. All thermal ellipsoids are set at the 90% probability level.

[*] Dr. C. Hoch
Institute for Inorganic Chemistry, University of Stuttgart
Pfaffenwaldring 55, 70569 Stuttgart (Germany)
E-mail: hoch@iac.uni-stuttgart.de
Prof. Dr. A. Simon
Max Planck Institute for Solid State Research
Heisenbergstrasse 1, 70569 Stuttgart (Germany)

[**] We thank Eva Brücher, Gisela Siegle, and Dr. Reinhard Kremer from Max Planck Institute for Solid State Research, Stuttgart, for the conductivity measurements. C.H. thanks Dr.-Leni-Schöninger-Stiftung for generous funding.

Supporting information for this article is available on the WWW under http://dx.doi.org/10.1002/anie.201108064.

hexagonal rod packing. Three crystallographically independent rods are present in the unit cell, around Na1, Na2, and Na3. They show almost identical topology and only differ in their respective surroundings (Figure 1b). The rod packing represents a 1/3 superstructure which is also visible in the diffraction pattern. A second superstructure with a hexagonal mesh of 1/13 of the real structure unit cell results from the distorted hexagonal closest packing of Na and Hg atoms. A view of the unit cell and the diffraction pattern of the *hk*0 plane with the underlying set of two different quasi-hexagonal subcells is shown in Figure 2.

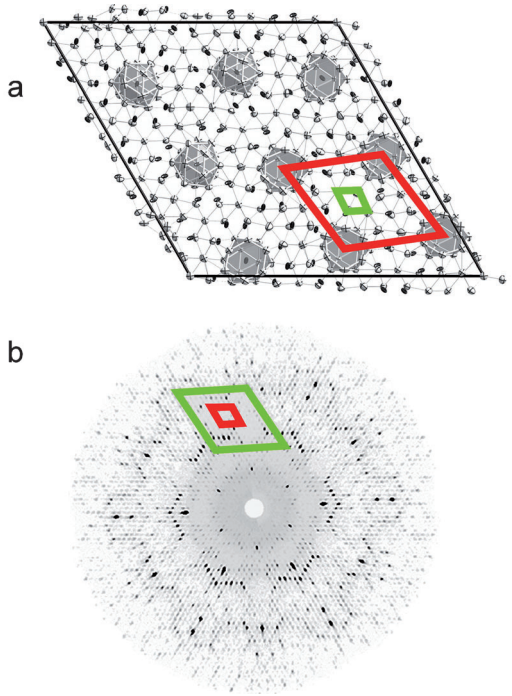

Figure 2. a) Projection on the unit cell of $Na_{11}Hg_{52}$ parallel to the *c* axis. The fine lines depict the distorted hexagonal closest sphere packing of Na and Hg atoms (small green 1/13 subcell), the gray polyhedra depict the distorted hexagonal closest rod packing (red 1/3 subcell). All ellipsoids are set at 90% probability. b) Diffraction pattern (*hk*0 plane). The corresponding reciprocal supercells to the subcells in Figure 2a are outlined in red and green, and the actual *a***c** unit mesh is given by the hexagonal pattern defined by the weak reflections.

The diffraction patterns of the superstructures and the actual structure are tilted towards one another by 1/13. Again, this tilt is visible both in the real-space structure and the diffraction pattern. The Hg atoms have quite sharply defined first coordination spheres with Hg–Hg distances ranging from 275.6(8) pm (Hg76–Hg78) to 377.5(6) pm (Hg10–Hg10). The coordination polyhedra can be classified as centaur polyhedra (coordination number CN = 10), Edshammar polyhedra (CN = 11), and icosahedra (CN = 12). They can occur isolated or as face-sharing or interpenetrating double polyhedra. In addition, some polyhedra with CN = 13 or 14 are found. Representatives of these polyhedra are compiled in Figure 1a. The only case of a monocapped Edshammar polyhedron (CN = 12) is the surrounding for Hg89, which is one of three out of 102 Hg atoms having only Hg and no Na atoms in their first coordination spheres: Hg89, Hg100, and Hg102 (the latter two are coordinated by 11 Hg atoms in Edshammar polyhedra).

In the complex structure of $Na_{11}Hg_{52}$ yet another feature of complexity enters with these polyhedra composed only of Hg. In the case of Hg89, a considerable mixed occupation with the refined ratio Hg:Na = 0.48(2) is found, common to all the crystals studied from different batches and measured at different temperatures. On the position of Hg100 a much lower Na fraction (88(5)% Hg) is found, and on the position of Hg102 no significant mixed occupation was observed. The mixed occupation occurs only in those cases where Hg atoms are coordinated only by other Hg and no Na atoms, and the most pronounced mixed occupation is found for the Hg atom with the largest coordination polyhedron. This results in the refined sum formula $Na_{11+x}Hg_{52-x}$ with $x = 0.19$.

The extraordinary complexity of this crystal structure can be rationalized in a model utilizing a newly developed mathematical approach[18] which simplifies the structure description by considerably reducing the amount of parameters in a slightly idealized picture. Work on a detailed report on this approach to structure descriptions based on number theory is in progress.

$Na_{11}Hg_{52}$ shows the typical behavior of a "bad" metal. As depicted in Figure 3, the metallic conductivity is combined with an especially low limit resistance. Following the Ioffe–

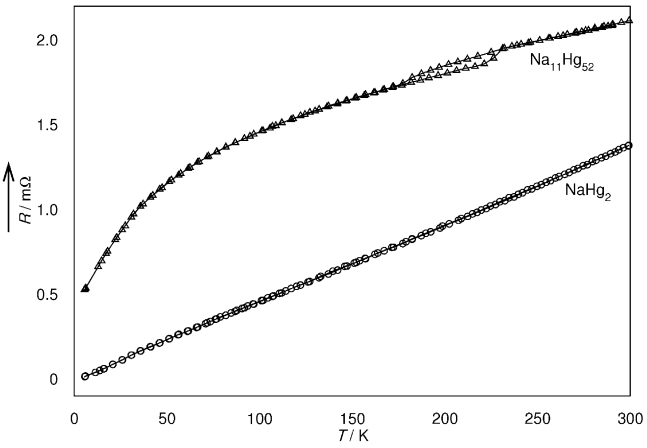

Figure 3. Temperature dependence of the electrical resistance of $Na_{11}Hg_{52}$ and $NaHg_2$. Heating and cooling curves are plotted for both amalgams ($Na_{11}Hg_{52}$: triangles, $NaHg_2$: circles). The curves for $Na_{11}Hg_{52}$ show the additional effect of freezing and melting of a very thin surface film of elemental mercury with a large hysteresis.

Regel law,[19] this behavior can be interpreted as being due to a small scattering length of the conducting electrons because of the long translational period in this low-symmetric structure with a large unit cell. The amalgam $NaHg_2$ with AlB_2 structure also shows metallic behavior, but the limit resistance only influences the thermal dependence of the conductivity at much higher temperature.

Alkali-metal amalgams with high Hg content are model systems for structures with polar metal–metal bonding. The

competitive interplay of three chemical bonding principles forms a structure of extremely high complexity. Only a few examples of binary compounds with such large unit-cell volumes are known, most of them of high symmetry[20] (e.g. Rb_8Sn_{44} and Cs_8Sn_{44} in the clathrate-I structure type).[21] Others demonstrate highly polar intermetallic structure types in the sense of Zintl phases (e.g. $Cs_{52}Sn_{82}$,[22] $K_{12}Si_{17}$,[23] and $K_{17}In_{41}$,[24]) or representatives of approximations for quasi-crystalline structures (e.g. the Samson phases β-Mg_2Al_3 and Cd_3Cu_4, $Ca_{13}Cd_{76}$, or $Ta_{97}Te_{60}$).[25]

The structural motif of a hexagonal closest packing of Na and Hg metal atoms which differ only by less than 10% in their respective atomic radii can clearly be discerned in the structure of $Na_{11}Hg_{52}$ and is typical for structures with metallic bonding. However, this feature is remarkable as the large difference in the respective electronegativities of Na and Hg suggests an electron transfer from Na to Hg resulting in strong Coulomb interactions between Na^+ ions with a considerably smaller ionic radius and a negatively charged Hg sublattice. Clearly, the electron transfer is incomplete in the case of the Na amalgam, in contrast to amalgams of K, Rb, or Cs.[26] The same holds for the aurides *A*Au (*A* = Na, K, Rb, Cs)[27] where metallic behavior and hence incomplete electron transfer is found for NaAu, but complete electron transfer can be detected in the red transparent crystals of CsAu. Nevertheless, the electron transfer is pronounced enough that the resulting Coulomb interactions between the negatively polarized Hg sublattice and the positively polarized Na atoms lead to the formation of Hg coordination polyhedra around Na and vice versa. The third building principle results from the tendency of negatively polarized Hg atoms to behave as a p-block metal with a low valence-electron concentration and the tendency to cluster formation with metal–metal bonds.[28] In mercury-rich alkali-metal amalgams these three influences are in a delicate balance and cause high complexity as well as the typical "bad" metal character, making them ideal model structures for studies on polar metallic behavior.

Experimental Section

When a small portion of metallic sodium is added to an excess of liquid mercury, $NaHg_2$ is formed with a flash, and mercury (boiling point: 630 K) evaporates. Annealing a mixture of $NaHg_2$ and Hg (with a small excess of Hg) just below the peritectic decomposition temperature of 157°C[15] does not yield the desired product over a period of weeks due to kinetic problems in nucleus formation.

However, electrolyzing a solution of dry NaI in *N*,*N*-dimethylformamide at 50°C with a drop of mercury suspended in an amalgamated copper spoon as cathode and a platinum foil as anode under argon atmosphere (Figure 4a) results in the formation of phase-pure $Na_{11}Hg_{52}$ in the form of dendritic crystals (Figure 4b, inset).

This method already has been shown to be a convenient synthetic approach towards amalgams with especially high mercury content and low peritectic decomposition temperatures.[29,30] The quality of these primary crystals is insufficient for X-ray structure analyses, but they can be used as seeds in the synthesis of $Na_{11}Hg_{52}$ from Hg and $NaHg_2$ as starting materials. Annealing $NaHg_2$ and Hg while oscillating the temperature by ±5°C just below 157°C in the presence of the $Na_{11}Hg_{52}$ seeds results in the consumption of $NaHg_2$ within minutes and growth of large crystals of $Na_{11}Hg_{52}$ of very high quality (Figure 4b). The starting material $NaHg_2$ can easily be prepared by allowing stoichiometric mixtures of sodium metal and mercury to react at 470°C under Ar.

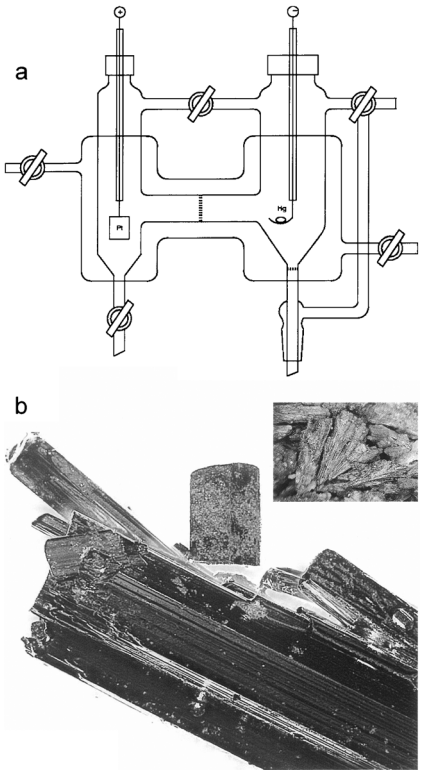

Figure 4. a) Schematic representation of the apparatus used for preparative isothermal electrolysis with strict exclusion of air and moisture. b) Crystals of $Na_{11}Hg_{52}$ (ca. 5-fold magnification) formed from a mixture of Hg and $NaHg_2$ using the dendritic crystals from the electrolysis of NaI in *N*,*N*-dimethylformamide on a Hg cathode (top right inset, ca. 30-fold magnification) as seeds.

Received: November 16, 2011
Published online: January 10, 2012

Keywords: amalgams · mercury · polar metals · sodium · structure elucidation

[1] http://www.eurochlor.org.
[2] T. F. O'Brien, T. V. Bommaraju, F. Hine, *Handbook of Chlor-Alkali Technology*, Springer, New York, **2005**.
[3] H. Y. Castner, US-Patent No. 528322, **1894**.
[4] I. Moussallem, J. Jörrisen, U. Kunz, S. Pinnow, T. Turek, *J. Appl. Electrochem.* **2008**, *38*, 1177–1194.
[5] Ministry of the Environment, Germany, Intergrated study on the avoidance and reduction of environmental polution (IVU): Reference document concerning the best available techniques of the chlor-alkali industry, http://www.bvt.umweltbundesamt.de/archiv/chloralkaliindustrie.pdf, **2001**.
[6] Paris Commission, Reducing atmospheric emissions from existing chlor-alkali plants, PARCOM Decision 90/3, Reykjavik, **1990**.
[7] Eurochlor, *Chlorine Industry Review 2009–2010*, http://www.eurochlor.org, **2011**.
[8] L. D. Hylander, M. Meili, *Crit. Rev. Environ. Sci. Technol.* **2005**, *35*, 1–36.

[9] A. A. Lindley, An economic and environmental analysis of the chlor-alkali production process: Mercury cells and alternative technologies in: European Comission, Directorate-General III Industry, C-4, Chemicals, plastics, rubber **1997**.

[10] R. G. Adams, T. V. Bommaraju, S. D. Fritts, US-Patent No. 5262133, **1993**.

[11] J. J. Berzelius, M. M. Pontin, *Gilb. Ann. Phys.* **1807**, *3*, 269 – 304.

[12] H. Davy, *Philos. Trans. R. Soc. London* **1808**, *98*, 1 – 44.

[13] J. W. Nielsen, N. C. Baenziger, *Acta Crystallogr.* **1954**, *7*, 277 – 282.

[14] D. Toelstede, PhD Thesis, University of Siegen (Germany) **1991**.

[15] *Binary Phase Diagrams* (Ed.: T. B. Massalski), American Society for Metals, Metals Park, Ohio, **1987**.

[16] Crystal structure data for $Na_{11}Hg_{52}$ at $T = 295(2)$ K: hexagonal, space group $P\bar{6}$ (No. 174), $a = 39.703(2)$, $c = 9.6810(5)$ Å, $V = 13216(1)$ Å^3, $Z = 9$, $\rho = 12.043$ g cm^{-3}; diffractometer: STOE IPDS1 ($Ag_{K\alpha}$ radiation, graphite monochromator); $\mu(Ag_{K\alpha}) = 73.784$; $2\theta_{max} = 32.00°$; 62054 observed intensities, 9456 unique; Lorentz, polarization and numerical absorption correction;[31] least-squares refinement on I (all atoms anisotropic, common set of U_{ij} for all Na atoms) with SHELXL97;[32] 836 free variables, R values ($I \geq 2\sigma(I)$): $R1 = 0.0475$, $wR2 = 0.1075$; max./min. residual electron density: $+3.42/-3.12$ e Å^{-3}. Further details on the crystal structure investigations may be obtained from the Fachinformationszentrum Karlsruhe, 76344 Eggenstein-Leopoldshafen, Germany (fax: (+49) 7247-808-666; e-mail: crysdata@fiz-karlsruhe.de), on quoting the depository number CSD-421584.

[17] a) H. J. Deiseroth, D. Toelstede, W. Bauhofer, *Z. Anorg. Allg. Chem.* **1990**, *587*, 103 – 109; b) H. J. Deiseroth, A. Stupperich, R. Pankaluoto, N. E. Christensen, *Z. Anorg. Allg. Chem.* **1991**, *597*, 41 – 50; c) H. J. Deiseroth, M. Rochnia, *Angew. Chem.* **1993**, *105*, 1556 – 1558; *Angew. Chem. Int. Ed. Engl.* **1993**, *32*, 1494 – 1495; d) H. J. Deiseroth, M. Rochnia, *Z. Anorg. Allg. Chem.* **1994**, *620*, 1736 – 1740; e) A. V. Tkachuk, A. Mar, *Acta Crystallogr. Sect. E* **2006**, *62*, i129 – i130.

[18] W. Hornfeck, B. Harbrecht, *Acta Crystallogr. Sect. A* **2009**, *65*, 532 – 542.

[19] A. F. Ioffe, A. R. Regel in *Prog. Semicond.*, *Vol. 4* (Eds.: A. F. Gibson, F. A. Kroger, R. E. Burgess), Heywood, London, **1960**, p. 237.

[20] J. Dshemuchadse, D. Y. Jung, W. Steurer, *Acta Crystallogr. Sect. B* **2011**, *67*, 269 – 292.

[21] a) J. T. Zhao, J. D. Corbett, *Inorg. Chem.* **1994**, *33*, 5721 – 5726; b) H. G. von Schnering, R. Kröner, M. Baitinger, K. Peters, R. Nesper, Yu. Grin, *Z. Kristallogr. New Cryst. Struct.* **2000**, *215*, 205 – 206; A. Kaltzoglou, T. Fässler, M. Christensen, S. Johnsen, B. Iversen, I. A. Presniakov, A. Sobolev, A. Shevelkov, *J. Mater. Chem.* **2008**, *18*, 5630 – 5637.

[22] C. Hoch, M. Wendorff, C. Röhr, *Z. Anorg. Allg. Chem.* **2003**, *629*, 2391 – 2397.

[23] C. Hoch, M. Wendorff, C. Röhr, *J. Alloys Compd.* **2003**, *361*, 206 – 221.

[24] G. Cordier, V. Müller, *Z. Naturforsch. B* **1994**, *49*, 721 – 728.

[25] a) S. Samson, *Acta Crystallogr.* **1965**, *19*, 401 – 413; S. Samson, *Acta Crystallogr.* **1967**, *23*, 586 – 600; b) M. Conrad, B. Harbrecht, *Chem. Eur. J.* **2000**, *8*, 3094 – 3102; c) C. Pay Gómez, S. Lidin, *Angew. Chem.* **2001**, *113*, 4161 – 4163; *Angew. Chem. Int. Ed.* **2001**, *40*, 4037 – 4039.

[26] a) E. J. Duwell, N. C. Baenziger, *Acta Crystallogr.* **1955**, *8*, 705 – 710; b) E. J. Duwell, N. C. Baenziger, *Acta Crystallogr.* **1960**, *13*, 476 – 479; c) E. Biehl, H. J. Deiseroth, *Z. Anorg. Allg. Chem.* **1999**, *625*, 1337 – 1342; d) E. Biehl, H. J. Deiseroth, *Z. Anorg. Allg. Chem.* **1999**, *625*, 1073 – 1080; e) E. Todorov, S. C. Sevov, *J. Solid State Chem.* **2000**, *149*, 419 – 427; f) H. J. Deiseroth, A. Strunck, *Angew. Chem.* **1989**, *101*, 1286 – 1287; *Angew. Chem. Int. Ed. Engl.* **1989**, *28*, 1251 – 1252; g) E. Biehl, H. J. Deiseroth, *Z. Anorg. Allg. Chem.* **1999**, *625*, 389 – 394; h) H. J. Deiseroth, A. Strunck, W. Bauhofer, *Z. Anorg. Allg. Chem.* **1989**, *575*, 31 – 38; i) H. J. Deiseroth, A. Strunck, *Angew. Chem.* **1987**, *99*, 701 – 702; *Angew. Chem. Int. Ed. Engl.* **1987**, *26*, 687 – 688.

[27] a) E. Zintl, J. Goubeau, W. Dullenkopf, *Z. Phys. Chem. Abt. A* **1931**, *154*, 1 – 46; b) W. E. Spicer, A. H. Sommer, J. G. White, *Phas. Rev.* **1959**, *115*, 57 – 62; c) G. A. Tinelli, D. F. Holcomb, *J. Solid State Chem.* **1978**, *25*, 157 – 165.

[28] J. Köhler, M.-H. Whangbo, *Solid State Sci.* **2008**, *10*, 444 – 449.

[29] C. Hoch, A. Simon, *Z. Anorg. Allg. Chem.* **2008**, *634*, 853 – 856.

[30] C. Hoch, A. Simon, *Z. Anorg. Allg. Chem.* **2006**, *632*, 2288 – 2294.

[31] a) Stoe & Cie., Darmstadt, Germany, *X-AREA V. 1.39* (**2006**); b) Stoe & Cie., Darmstadt, Germany, *X-SHAPE V- 2.07* (**2005**); c) Stoe & Cie., Darmstadt, Germany, *X-RED V. 1.31* (**2005**).

[32] G. M. Sheldrick, *Acta Crystallogr. Sect. A* **2008**, *64*, 112 – 122.

[33] L. M. Gelato, E. Parthé, *J. Appl. Crystallogr.* **1987**, *20*, 139 – 143.

[34] H. D. Flack, *Acta Crystallogr. Sect. A* **1983**, *39*, 876 – 881.

